Triple-decker complexes comprising heterocyclic middle-deck with coinage metals

Chandan Nandi, Ranjit Bag, Soumen Giri, Arindam Roy, Marie Cordier, Sundargopal Ghosh

Research Highlights

- Syntheses and structural characterization of group 9 triple decker sandwich complexes comprising a planar 5-membered middle-deck with coinage metal.
- Density functional theory calculations provided a well-defined picture about the bonding of these heterometallic triple decker complexes.
- The experimental results have been accompanied and rationalized using DFT studies.

Triple-decker complexes comprising heterocyclic middle-deck with coinage metals

Chandan Nandi,[a] Ranjit Bag,[a] Soumen Giri,[a] Arindam Roy,[a] Marie Cordier,[b] and Sundargopal Ghosh*[a]

[a] *Department of Chemistry, Indian Institute of Technology Madras, Chennai 600 036, India*
Email : sghosh@iitm.ac.in

[b] *Univ Rennes, CNRS, Institut des Sciences Chimiques de Rennes, UMR 6226, F-35000 Rennes, France*

Keywords: cobalt, rhodium, metallaheteroborane, triple-decker, copper

ABSTRACT

Earlier accounts of triple-decker complexes comprising main group elements and transition metals in the middle-deck, motivated us to synthesize triple-decker complexes containing coinage metals in the middle-deck. As a result, we have explored the reactivity of open-cage *nido*-[(Cp*M)$_2$\{μ-$B_2H_2E_2$\}], **1**-**3** (Cp* = η^5-C_5Me_5, **1**: M = Co, E = S; **2**: M = Co, E = Se; **3**: M = Rh, E = Se) with [CuBr(SMe_2)]. All the reactions yielded triple-decker complexes, [(Cp*M)$_2$\{μ-$B_2H_2E_2$CuBr\}], **4**-**6** (**4**: M = Co, E = S; **5**: M = Co, E = Se; **6**: M = Rh, E = Se) having [CuBr] in the middle-deck. The removal of the SMe_2 ligand resulted in the formation of complexes **4**-**6** as a single product. These complexes are examples of triple-decker species having a planar 5-membered [B_2E_2Cu] (E = S or Se) middle deck, in which the Cu exists as Cu(I) with an elongated M-Cu bonding interaction. Synthesized complexes have been established by ESI-MS, multinuclear nuclear

magnetic resonance (NMR), and IR spectroscopy. The solid-state structures of **5** and **6** were confirmed by single-crystal X-ray diffraction analyses. Density functional theory (DFT) analyses of these complexes have presented a high electron donation from the $[B_2E_2]$ (E = S or Se) fragment of the middle ring to the axial metals and a weak bonding interaction between group 9 metals and Cu.

1. Introduction

Since the discovery of ferrocene in 1951,[1] the quest for novel sandwich complexes have been a significant area of study in the field of organometallic chemistry due to their fascinating physical and chemical characteristics as well as their distinctive structural features.[2] Syntheses of metallocenes with the increasing number of rings and metals led to triple- and multi-decker sandwich complexes which contain heterocyclic rings simultaneously bonded to two or more oppositely lying transition-metals.[3] Triple-decker complexes comprising a planar or bent middle ring are extremely versatile and exhibit significant unpaired electron delocalization between metal centers.[4-7] The possibility of the existence of a triple-decker sandwich complex was first pointed out by Salzer and Werner in 1972 after the discovery of $[Ni_2Cp_3]^+$ (Cp = η^5-C_5H_5).[8] Grimes and coworkers have isolated the first structurally characterized triple-decker complex, $[(CpCo)_2RC_2B_3H_4]$ (R = H/Me) (Chart 1, **I**).[9] However, compared to triple-decker complexes with carbocyclic ligand systems, such complexes with solely inorganic ring systems or heterocyclic ligands are still comparatively understudied due to a lack of effective synthetic methods. In 1982, Rheingold and coworkers reported the first triple-decker complex, $[(CpMo)_2(\mu,\eta^4\text{-}As_5)]$ (**II**) having *cyclo*-As_5 moiety in middle-deck.[10] Later, in 1986, Scherer and coworkers isolated $[(CpCr)_2(\mu,\eta^5\text{-}P_5)]$ (**III**), the first triple-decker complex in which a *cyclo*-P_5 unit was stabilized as middle-deck.[11] Fehlner and coworkers have isolated a triple-decker complex comprising *open*-B_5

moiety as middle-deck [$(Cp^*ReH)_2B_5Cl_5$] (**IV**), which is the first example of a dimetallaborane fully chlorinated at boron.[12] Kudinov and coworkers have reported a few triple-decker complexes of iron, ruthenium, and molybdenum, such as [$Cp^*Fe(\mu,\eta^5{:}\eta^5\text{-}P_5)MCp^*]^+$ (M = Fe, Ru) and [$(C_7H_7)Mo(\mu,\eta^5{:}\eta^5\text{-}P_5)FeCp^*]^+$.[13] Scheer and coworkers have isolated several unique neutral triple-decker sandwich complexes having functionalized *cyclo*-P_5 moieties as middle-decks by using [$Cp^*Fe(\eta^5\text{-}P_5)$] as starting material.[14] Recently, the same group has reported a new high-yielding synthetic method for triple-decker complex [$Cp^*Fe(\mu,\eta^5{:}\eta^5\text{-}P_5)Mo(CO)_3$] (**V**).[15] Very recently, Roesky and coworkers have reported trinuclear triple-decker complexes with P_5 or As_5 middle-decks and a planar lead containing heterocycle as a lower deck that disclosed the first heterotrimetallic Pb-Fe-Li triple-decker polypnictogenides.[16]

However, the development of such heterometallic systems that incorporate main group elements, semi-metals, and transition metals in the middle-deck are still relatively unexplored due to the lack of efficient synthetic routes. Although several triple-decker complexes having homocyclic ring composed of carbon, boron, phosphorus, and arsenic as middle-decks are known in the literature, heterocyclic ring systems as middle-decks are still limited.[17] As a result, syntheses of triple-decker complexes having coinage metal (*i.e.*, Cu) in the middle-deck became of interest. Coinage metal complexes have attracted a lot of attention due to their striking structural features and find prospective uses in various fields, particularly in nanotechnology.[18] Among several metallic nanoclusters, group 11 coinage metals have drawn significant interest and show different physio-chemical properties like luminescence, non-linear optical response, and molecular chirality.[19]

(Chart 1. near here)

As part of our research on such complexes,[20-22] we have recently synthesized and characterized triple-decker complexes [(Cp*M)$_2${$B_2H_2E_2Pd(Cl)_2$}] (E = S and Se; M = Rh, Co, or Ir) comprising {$PdCl_2$} moiety in the middle-deck.[22] Very recently, we have isolated a triple-decker sandwich complex of titanium [(Cp*Ti)$_2$(μ-η^6:η^6-B_6H_6)(μ-H)$_6$] containing a nearly planar [B_6H_6] ring sandwiched between two {Cp*Ti} fragments.[20c] As a result, the isolation of triple-decker complexes comprising planar middle-deck following a high-yielding synthetic route became appealing. In this article, we have revisited the chemistry of group 9 transition metal complexes, [(Cp*M)$_2${μ-$B_2E_2H_2$}] (M = Co, or Rh; E = S or Se) containing chalcogen atoms at the open site, with [CuBr(SMe_2)]. Herein, we have reported syntheses, structures, and bonding of triple-decker complexes having a planar heterocyclic 5-membered middle-deck.

2. Results and discussion

Syntheses and characterization of triple-decker complexes, 4-6. Cluster expansion reactions of preformed metallaheteroboranes and metallaboranes by incorporating main group and metal fragments afforded clusters of both unusual shape and electron count.[23-25] However, syntheses of triple-decker complexes with planar middle-decks consisting of transition metals or main group elements are rare besides a few instances, including the first complex [(Cp*Re)$_2${μ-η^6:η^6-$B_4H_4Co_2(CO)_5$}].[4b,25e] As a result, we have studied the reactivity of open-core triple-decker complexes *nido*-[(Cp*M)$_2${μ-$B_2H_2E_2$}], **1**-**3** (**1**: E = S, M = Co; **2**: E = Se, M = Co; **3**: E = Se, M = Rh) with [CuBr(SMe_2)]. As shown in Scheme 1, the reactions of **1**-**3** with [CuBr(SMe_2)] at room temperature yielded **4**-**6**, respectively. Immediately after the addition of [CuBr(SMe_2)] with **1** and **2**, the reaction mixtures changed to green due to the formation of **4** and **5**. In contrast, the reaction mixture changed to red for **6**. Note that all the complexes have been isolated as a single-product in good yields. The formation of **4**-**6** from **1**-**3** may be described as metallo-ligand approach, in which

1-**3** act as a ligand to the {CuBr} unit. From the reaction mixtures, SMe_2 was removed by washing with hexane, and products were characterized without further purification. Although the reactions of [Ag(PPh_3)Cl] and [AuCl(SMe_2)] with **1** and **2** yielded almost immediately blue color species, they converted back to starting materials **1** and **2** within two hours, respectively. As a result, we are not able to isolate and structurally characterize the Ag and Au analogues of **4** and **5**, respectively.

(Scheme 1. near here)

All complexes **4**-**6** were characterized by NMR, ESI-MS, and IR spectroscopy. The ^{1}H NMR spectra of **4**-**6** show singlet chemical shifts at δ = 1.60, 1.77, and 1.77 ppm, respectively which are due to Cp* ligands. The presence of BH terminal protons were confirmed by $^{1}H\{^{11}B\}$ NMR spectra that showed chemical shifts at δ = 4-6 ppm. The $^{11}B\{^{1}H\}$ NMR spectra show one boron peak at δ = 20.0 ppm for **4**, 18.1 ppm for **5**, and 17.9 ppm for **6**. Further, the presence of Cp* ligands for **4**-**6** were also confirmed by $^{13}C\{^{1}H\}$ NMR spectra. The IR spectra of all these complexes display peak for BH_t in the region of ~ 2511-2500 cm^{-1}. The ESI-MS spectra show isotopic patterns at *m/z* = 580.0348 $[M\text{-}Br+CH_3CN]^+$ for **4**, 675.9225 $[M\text{-}Br+CH_3CN]^+$ for **5**, and 763.8659 $[M\text{-}Br+CH_3CN]^+$ for **6** [M = $C_{20}H_{32}B_2Co_2S_2CuBr$ (**4**), $C_{20}H_{32}B_2Co_2Se_2CuBr$ (**5**), and $C_{20}H_{32}B_2Rh_2Se_2CuBr$ (**6**)]. All the spectroscopic data, along with mass spectrometric data, suggest comparable structures for **4**-**6**. Finally, the single-crystal X-ray diffraction analyses were performed to determine the solid-state structures of **5** and **6**.

(Fig. 1. near here)

The single-crystals of **5** and **6** were grown by slow evaporation of CH_2Cl_2 solution of the complexes at −5 °C. Unfortunately, we are not able to get good quality single crystals for **4**. The

solid-state structures of **5** and **6**, shown in Fig. 1, correspond to triple-decker complexes where group 9 metals (Co/Rh) are sandwiched between five-membered [B_2E_2Cu] ring and Cp* ligands. Middle-decks in **5** and **6** have slightly deviated from coplanarity with a dihedral tilt angle stretched from 1.95°-5.02° (Fig. 2), in which the deviation is maximum for **6**. The bridging ligands in **5** and **6** contain a five-membered [B_2E_2Cu] ring in which Cu(I)Br unit bind through chalcogen atom with a bite angle of ~96°. Interestingly, the bromine atom and chalcogen atoms in **5** and **6** are in a trigonal planar arrangement with Cu(I), while the axial group 9 metals are weakly coordinated with Cu(I). The B-B bond distance of **5** (1.69(2) Å) and **6** (1.680(13) Å) are shorter than that of *nido*-**2** (1.726(7) Å)[26] and *nido*-**3** (1.739(4) Å),[27] respectively (Table 1). While the average B-Se distances of **5** (1.993 Å) and **6** (2.001 Å) are longer than that of *nido*-**2** (1.985(6) Å],[16] and *nido*-**3** (1.983(3) Å)[27]. The average Cu-Se distances of **5** (2.376 Å) and **6** (2.381 Å) are compared to that of {Cu[Se(2,4,6-$^{i}Pr_3C_6H_2$)]}$_6$ (2.370(2) to 2.412(2) Å).[28] The average Co-Cu distance in **5** (2.676(2) Å) is considerably longer (~0.3 Å) as compared to binuclear Cu-Co complex, [(tmed)CuCo(CO)$_4$] ($d_{Cu\text{-}Co}$ = 2.379 (1) Å; tmed = N,N,N',N'-tetramethylethylenediamine).[29] Similarly, the average Rh-Cu distance in **6** (2.777(2) Å) is longer as compared to Rh-Cu complex, [RhCu(PPh_3)(cod)(η^5-7,8-$C_2B_9H_9Me_2$)] ($d_{Rh\text{-}Cu}$ = 2.633(2) Å, cod = cycloocta-1,5-diene).[30] Complexes 4-**6** can be described as 60 cluster valance electrons (CVE) and 8 SEP: [2{Cp*M} + 2{BH}+ 2{E} + {CuBr}] = [2{2} + 2{2} + 2{4} +{0}]/2 = 8 SEP] triple-decker complexes with a pentagonal bipyramidal geometry.

(Fig. 2. near here)

(Table 1. near here)

The DFT analyses of **5** and **6** have been carried out using the Gaussian 16 program at the BP86/def2- TZVP level of theory to understand the structures and bonding of such triple-decker complexes. The optimized geometrical parameters of **5** and **6** are in accordance with their solid-state structural parameters (Table S1). Additionally, the GIAO-DFT (gauge-including atomic orbitals-density functional theory) calculated ^{11}B chemical shift values of **5** and **6** are also in good agreement with the values observed experimentally (Table 1). The frontier molecular orbital analyses of **5** and **6** display a lower HOMO-LUMO gap in **5** (~ 1.269 eV) compared to **6** (~1.379 eV). This may be due to the presence of different axial metals (Co or Rh) in their framework. The HOMOs of **5** and **6**, shown in Fig. 3, are significantly concentrated over the axial metals (Co or Rh; d-orbitals), Se (p-orbitals), Cu (d-orbitals), and Br (p-orbital) atoms. In contrast, the LUMOs are mainly localized on the axial metals (d-orbitals) and Se atoms (p-orbitals). Further, the HOMO-12 of **5** and HOMO-14 of **6** (Fig. 3) show σ bonding interactions between the axial metals and Cu through d-orbitals. The M-Cu Wiberg bond indices (WBI) for **5** and **6** (~0.14) suggest weak bonding interaction between group 9 metals and Cu. Further, the WBI suggests a weaker Cu-Se (~0.36) bond as compared to the Cu-Br (~0.71) bond. The WBI of B-B and B-Se in **5** and **6** indicate strong bonding interactions. However, the M-M Wiberg bond indices (~0.06) for **5** and **6** indicate the absence of a bonding interaction between two axial metal centers (Table S1). The natural charges obtained from NBO (natural bond orbital) analyses, shown in Table S3, display positive and negative charges on selenium and boron atoms, respectively, that indicate their donating nature towards metals.

(Fig. 3. near here)

The topological analyses of **5** and **6** were carried out using QTAIM method to reveal the interaction of the axial group 9 transition metals (Co/Rh) with the middle-deck. The positive value of $\nabla^2\rho(r)$ (Laplacian of the electron density) at the bond critical points of M-Se, Cu-Br, and M-B, reveal electron-donating nature of these ligands towards metals (Table 2). Additionally, the topological properties show that the Cu-Se bonds are more electrostatic than the Co-E or Rh-E bonds (E = S or Se). Furthermore, the electron localization function (ELF) values, negative $\nabla^2\rho(r)$, and negative H(r) values along the B-B and B-Se bonds suggest the pure covalent character of these bonds. These variations are observed in the contour map of the $\nabla^2\rho(r)$, shown in Fig. 4(a), in the [CuB_2Se_2] middle-deck for **5**. For instance, the electron concentration is higher between Se1-B1-B2-Se2 bonds, while the electron density is lower between Cu-Se bonds. In addition, the topology analysis for **5**, shown in Fig. 4(b), suggests the 3c-2e interaction between the axial metals and B-B bond.

(Table 2. near here)

(Fig. 4. near here)

3. Conclusion

In summary, we have isolated and structurally characterized triple-decker sandwich complexes of group 9 metals having planar 5-membered [CuB_2Se_2] ring in the middle-deck. The reported methodology is an efficient route for the generation of heterometallic triple-decker complexes with high yields. Interestingly, complexes **4-6** are the first examples of triple-decker complexes comprising coinage metal in the middle-deck. Further, theoretical calculations gave insight into the bonding of such complexes, in which the middle-deck is strongly bonded with the axial metals through the [B_2E_2] fragment. In contrast, a weak bonding interaction was observed between Cu

and the axial group 9 metals. Besides the syntheses of such heterotrinuclear triple-decker complexes, the usefulness of these complexes is under investigation.

4. Experimental section

General procedures and instrumentation. All the syntheses were executed under Ar atmosphere by using standard Schlenk line techniques. Tertrahydofuran, toluene, DCM (dichloromethane) and hexane were distilled under an argon atmosphere. All reagents, such as Cp*H, $RhCl_3$, $CoCl_2$, *n*-BuLi in hexane, [$LiBH_4$·THF] were purchased from Sigma Aldrich and used without purification. [$CuBr(SMe_2)$],[31] and **1**-**3**[26,32] were synthesized by following the literature procedures. All ^1H, $^{11}B\{^1H\}$ and $^{13}C\{^1H\}$ NMR spectra for the synthesized complexes were recorded on 500 or 400 MHz Bruker FT-NMR spectrometers. The residual solvent protons ($CDCl_3$, δ = 7.26 ppm) and carbon (δ = 77.1 ppm, $CDCl_3$) were employed as a reference for the ^1H and $^{13}C\{^1H\}$ NMR spectra, respectively. $^{11}B\{^1H\}$ spectra of all compounds were processed with a backward linear prediction algorithm to remove the broad $^{11}B\{^1H\}$ background signal of the NMR tube.[33] Qtof Micro YA263 HRMS and 6545 Qtof LC/MS instruments were used to record the mass of the compounds. IR spectra were recorded on a JASCO FT/IR-1400 spectrometer in dichloromethane solvent.

Syntheses of 4 and 5: In a flame-dried Schlenk tube, the deep blue solution of [$(Cp^*Co)_2B_2H_2S_2$], **1** (0.03 g, 0.06 mmol) and [$CuBr(SMe_2)$] (0.012 g, 0.06 mmol) in toluene (10 ml) was stirred at room temperature. The reaction mixture was changed from blue to green within 1 min and allowed to stir at room temperature for an additional 1 h. After filtration, the solvent was dried under vacuum and the residue was purified by washing with hexane, yielded a green solid, **4** [$(Cp^*Co)_2B_2H_2S_2CuBr$] (yield: 90-92% for a set of experiments). Single crystals were grown by slow diffusion of dichloromethane solution of **4** in dichloromethane at −5 ºC.

By following same reaction conditions, $[(Cp^*Co)_2B_2H_2Se_2]$, **2** (0.03 g, 0.05 mmol), and $[CuBr(SMe_2)]$ (0.01 g, 0.05 mmol) afforded green solid **5**, $[(Cp^*Co)_2B_2H_2Se_2CuBr]$ (yield: 90−95% for a set of experiments). Single crystals were grown by slow diffusion of dichloromethane solution of **5** at −5 ºC.

4: ESI-MS (ESI^+): *m/z* calc. for $[C_{20}H_{32}B_2Co_2S_2CuBr\text{-}Br+CH_3CN]^+$: 580.0368, found: 580.0348; $^{11}B\{^1H\}$ NMR ($CDCl_3$, 160 MHz, 22 °C, ppm): δ = 20.0 (s, 2B); $^1H\{^{11}B\}$ NMR ($CDCl_3$, 500 MHz, 22 °C, ppm): δ = 1.60 (s, 30H, $C_5\underline{\mathit{Me}}_5$), 4.57 (s, $2BH_t$); $^{13}C\{^1H\}$ NMR ($CDCl_3$, 125 MHz, 22 °C, ppm): δ = 91.8 (s, $\underline{C}_5Me_5$), 10.1 (s, $C_5\underline{\mathit{Me}}_5$); IR (dichloromethane, cm^{-1}): $\tilde{\nu}_{exp}$ = 2511 (BH_t); $\tilde{\nu}_{cal}$ = 2537 (BH_t).

5: ESI-MS (ESI^+): m/z calc. for $[C_{20}H_{32}B_2Co_2Se_2CuBr\text{-}Br+CH_3CN]^+$: 675.9256, found: 675.9225; $^{11}B\{^1H\}$ NMR ($CDCl_3$, 160 MHz, 22 °C, ppm): δ = 18.1 (s, 2B); $^1H\{^{11}B\}$ NMR ($CDCl_3$, 500 MHz, 22 °C, ppm): δ = 1.77 (s, 30H, $C_5\underline{\mathit{Me}}_5$), 4.38 (s, $2BH_t$); $^{13}C\{^1H\}$ NMR ($CDCl_3$, 125 MHz, 22 °C, ppm): δ = 97.6 ($\underline{C}_5Me_5$, s), 10.2 (s, $C_5\underline{\mathit{Me}}_5$); IR (dichloromethane, cm^{-1}): $\tilde{\nu}_{exp}$= 2500 (BH_t); $\tilde{\nu}_{cal}$ = 2535 (BH_t).

Synthesis of 6: In a flame-dried Schlenk tube, the deep orange solution of $[(Cp^*Rh)_2B_2H_2Se_2]$, **3** (0.03 g, 0.045 mmol) and $[CuBr(SMe_2)]$ (0.009 g, 0.045 mmol) in toluene (10 ml) was stirred at room temperature. The reaction mixture was changed from orange to red within 5 min and was allowed to stir at room temperature for an additional 1 h. After filtration, the solvent was dried under vacuum, and the residue was purified by washing with hexane, yielded a red solid, **6** $[(Cp^*Rh)_2B_2H_2Se_2CuBr]$ (yield: 95%). Single crystals were grown by slow diffusion of dichloromethane solution of **6** at −5 ºC.

6: ESI-MS (ESI$^+$): *m/z* calculated for $[C_{20}H_{32}B_2Rh_2Se_2CuBr\text{-}Br+CH_3CN]^+$: 763.8702, found: 763.8659; $^{11}B\{^1H\}$ NMR ($CDCl_3$, 160 MHz, 22 °C, ppm): δ = 17.9 (s, 2B); $^1H\{^{11}B\}$ NMR ($CDCl_3$, 500 MHz, 22 °C, ppm): δ = 1.77 (s, 30H, $C_5\underline{\textit{Me}}_5$), 5.7 (s, $2BH_t$); $^{13}C\{^1H\}$ NMR ($CDCl_3$, 125 MHz, 22 °C, ppm): δ = 90.8 (s, $\underline{C}_5Me_5$), 10.4 (s, $C_5\underline{\textit{Me}}_5$); IR (dichloromethane, cm^{-1}): $\tilde{\nu}_{exp}$= 2510 (BH_t); $\tilde{\nu}_{cal}$ = 2538 (BH_t).

Computational details: All the triple-decker complexes were optimized using the Gaussian 16[34] program at the BP86[35] functional along with def2-TZVP basis set from EMSL[36] Basis Set Exchange Library. The complexes were fully optimized starting from X-ray coordinates in the gaseous state (no solvent effect). Frequency calculations were carried out for the verification of the nature of the stationary state and to confirm the absence of any imaginary frequency, which eventually confirmed the minima on the potential energy hypersurface for all structures. NMR chemical shifts were computed by employing the gauge-including atomic orbitals (GIAOs) method[37] using the BP86/def2-TZVP optimized geometries. Chemical shifts corresponding to ^{11}B NMR were computed in relation to B_2H_6 (BP86 shielding constant for ^{11}B NMR: 80.9 ppm) and were then transformed to the standard [$BF_3.OEt_2$] scale by adding 16.6 ppm (the experimental δ (^{11}B) value of B_2H_6) to the computed values.[38] Wiberg bond indices (WBI)[39] were generated from natural bond orbital analysis (NBO)[40]. All the optimized geometries and orbital pictures were drawn by Chemcraft[41] visualization programs. Laplacian electronic distribution plots and two-dimensional electron density were generated using the Multiwfn package.[42]

X-ray structure determination analysis details: Suitable X-ray quality crystals for **5** and **6** were grown by slow diffusion of a hexane-CH_2Cl_2 solution at −5 ºC. The X-ray data were collected and integrated using a APEXII Bruker-AXS diffractometer for **5**, Bruker D8 VENTURE for **6,** and with graphite monochromated Mo-Kα (λ = 0.71073 Å) radiation at 150(2) K (for **5**), 296(2) K (for

6). The structures were solved using SHELXT-2014, SHELXS-97[43], and refined using SHELXL-2017, SHELXL-2018, SHELXL-2014,[44]. X-ray structures were drawn using Olex2[45]. CCDC-2150288 (**5**) and 2150289 (**6**) contain crystallographic data. These data can be obtained free of charge from the Cambridge Crystallographic Data Centre via www.ccdc.cam.ac.uk/data_request/cif.

Crystal data of **5**: $C_{20}H_{32}B_2BrCuCo_2Se_2$; formula weight, M_r.= 713.30; monoclinic; $P2_1/c$; unit cell, a = 13.978(3) Å, b = 10.317(2) Å, c = 17.313(3) Å, α = 90°, β = 90.131(9)°, γ = 90°; Z = 4; V = 2496.7(8) Å^3; μ = 6.678 mm^{-1}; F(000) = 1392; ρ_{calcd} = 1.898 g/cm^3; R_1 = 0.0631; wR_2 = 0.1373; 4721 independent reflections [2θ ≤ 51.36°], and 237 parameters.

Crystal data of **6**: $C_{20}H_{32}B_2BrCuRh_2Se_2$; formula weight, M_r.= 801.26; monoclinic; $P2_1/n$; unit cell, a = 11.0897(7) Å, b = 16.8608(12) Å, c = 14.0756(10) Å, α = 90°, β = 98.341(3)°, γ = 90°; Z = 4; V = 2604.0(3) Å^3; μ = 16.094 mm^{-1}; F(000) = 1536; ρ_{calcd} = 2.044 g/cm^3; R_1 = 0.0556; wR_2 = 0.1575; 4583 independent reflections [2θ ≤ 132.99°], and 264 parameters.

ACKNOWLEDGMENT

The authors acknowledge the Science and Engineering Research Board (SERB) (Project No. CRG/2019/001280), New Delhi, India, for financial support. C.N. thanks DST-INSPIRE and S.G. thanks the UGC for their research fellowships. The computational facility of IIT Madras is gratefully acknowledged.

Appendix A. Supplementary data

Supplementary data related to this article can be found at http://dx.doi.org.

REFERENCES

[1] T. J. Kealy, P. L. Pauson, Nature 168 (1951) 1039-1040.

[2] A. N. Nesmeyanov, N. S. Kochetkova, Russ. Chem. Rev. 43 (1974) 710–715.

[3] (a) W. Sibert, Russ. Chem. Rev. 60 (1991) 784-791; (b) R. B. King, Chem. Rev. 101 (2001) 1119-1152; (c) J. K. Burdett, E. Canadell, Organometallics 4 (1985) 805-815; (d) R. N. Grimes, Coord. Chem. Rev. 28 (1979) 47-96.

[4] (a) S. Ghosh, A. M. Beatty, T. P. Fehlner, J. Am. Chem. Soc. 123 (2001) 9188-9189; (b) K. Kawamura, M. Shang, O. Wiest, T. P. Fehlner, Inorg. Chem. 37 (1998) 608-609; (c) S. Ghosh, M. Shang, T. P. Fehlner, J. Am. Chem. Soc. 1999, 121, 7451-7452; (c) E. D. Jemmis, A. C. Reddy, Organometallics 7 (1988) 1561–1564.

[5] (a) A. N. Alexandrova, K. A. Birch, A. I. Boldyrev, J. Am. Chem. Soc. 125 (2003) 10786-10787; (b) A. N. Alexandrova, A. I. Boldyrev, H. J. Zhai, L. S. Wang, Coord. Chem. Rev. 250 (2006) 2811-2866; (c) J. W. Lauher, M. Elian, R. H. Summerville, R. Hoffmann, J. Am. Chem. Soc. 98 (1976) 3219–3224.

[6] W.-L. Li, L. Xie, T. Jian, C. Romanescu, X. Huang, L.-S. Wang, Angew. Chem. Int. Ed. 53 (2014) 1288-1292.

[7] B. P. T. Fokwa, M. Hermus, Angew. Chem. Int. Ed. 51 (2012) 1702-1705.

[8] (a) A. Salzer, H. Werner, Angew. Chem., Int. Ed. Engl. 11 (1972) 930−932; (b) H. Werner, Angew. Chem. Int. Ed. Engl. 16 (1977) 1-64.

[9] (a) D. C. Beer, V. R. Miller, L. G. Sneddon, R. N. Grimes, M. Mathew, G. J. Palenik,. J. Am. Chem. Soc. 95 (1973) 3046−3048; (b) R. N. Grimes, D. C. Beer, L. G. Sneddon, V. Miller, R. Weiss, Inorg. Chem. 13 (1974) 1138−1146; (c) R. N. Grimes, Coord. Chem. Rev. 28 (1979) 47−96.

[10] A. L. Rheingold, M.J. Foley, P. J. Sullivan, J. Am. Chem. Soc. 104 (1982) 4727-4729.

[11] O. J. Scherer, J. Schwalb, G. Wolmershauser, W. Kaim, R. Gross, Angew. Chem., Int. Ed. Engl. 25 (1986) 363–364.

[12] B. L. Guennic, H. Jiao, S. Kahlal, J. Y. Saillard, J. F. Halet, S. Ghosh, M. Shang, A. M. Beatty, A. L. Rheingold, T. P. Fehlner, J. Am. Chem. Soc. 126 (2004) 3203−3217.

[13] (a) A. R. Kudinov, M. I. Rybinskaya, Russ. Chem. Bull. 48 (1999) 1636–1642; (b) A. R. Kudinov, D. A. Loginov, Z. A. Starikova, P. V. Petrovskii, M. Corsini, P. Zanello, Eur. J. Inorg. Chem. 2002 (2002) 3018–3027; (c) A. R. Kudinov, P.V. Petrovskii, M. I. Rybinskaya, Russ. Chem. Bull. 48 (1999) 1374–1376.

[14] E. Mädl, E. V. Peresypkina, A. Y. Timoshkin, M. Scheer, Chem. Commun. 52 (2016) 12298–12301.

[15] M. E. Moussa, S. Welsch, L. Dütsch, M. Piesch, S. Reichl, M. Seidl, M. Scheer, Molecules 24 (2019) 325.

[16] X. Sun, A. K. Singh, R. Yadav, D. Jin, M. Haimerl, M. Scheer, P. W. Roesky, Chem. Commun. 58 (2022) 673–676.

[17] (a) T. Kuwabara, J.-D. Guo, S. Nagase, T. Sasamori, N. Tokitoh, M. Saito, J. Am. Chem. Soc. 136 (2014) 13059–13064; (b) M. Saito, N. Matsunaga, J. Hamada, S. Furukawa, M. Minoura, S. Wegner, J. Barthel, C. Janiak, Dalton Trans. 47 (2018) 8892–8896.

[18] (a) J. C. Garrison, W. J. Youngs, Chem. Rev. 105 (2005) 3978-4008; (b) C.K. Lee, C.S. Vasam, T. W. Huang, H. M. J. Wang, R. Y. Yang, C. S. Lee, I. J. B. Lin, Organometallics 25 (2006) 3768-3775. (c) A. Baghdasaryan, T. Burgi, Nanoscale, 13 (2021) 6283-6340.

[19] (a) X. Kang, M. Zhu, Chem. Soc. Rev. 48 (2019) 2422-2457; (b) J. Olesiak-banska, M. Waszkielewicz, M. Samoc. Phys. Chem. Chem. Phys. 20 (2018) 24523-24526.

[20] (a) A. Thakur, K. K. V. Chakrahari, B. Mondal, S. Ghosh, Inorg. Chem. 52 (2013) 2262-2264; (b) B. Mondal, K. Pal, B. Varghese, S. Ghosh, *Chem. Commun*. 51 (2015) 3828-3831; (c) S. Kar, S. Bairagi, A. Haridas, G. Joshi, E. D. Jemmis and S. Ghosh, Angew. Chem. Int. Ed. 61 (2022) e202208293.

[21] (a) B. Mondal, K. Pal, B. Varghese, S. Ghosh, Chem. Commun. 51 (2015) 3828−3831; (b) B. Mondal, M. Bhattacharyya, B. Varghese, S. Ghosh, Dalton Trans. 45 (2016) 10999−11007; (c) R. Bag, R. Prakash, S. Saha, T. Roisnel, S. Ghosh, Inorg. Chem. 60 (2021) 3524−3528; (d) K. Geetharani, B. S. Krishnamoorthy, S. Kahlal, S. M. Mobin, J. -F. Halet, S. Ghosh, Inorg. Chem. 51 (2012) 10176-10184.

[22] B. Joseph, R. Prakash, R. Bag, S. Ghosh. Inorg. Chem. 59 (2020) 16272-16280.

[23] (a) S. Ghosh, B. C. Noll, T. P. Fehlner, Dalton Trans. (2008) 371−378; (b) S. Ghosh, B. C. Noll, T. P. Fehlner, Angew. Chem., Int. Ed. 44 (2005) 6568−6571; (c) S. Kar, A. N. Pradhan, S. Ghosh, Polyhedral Metallaboranes and Metallacarboranes. In: Comprehensive

Organometallic Chemistry IV; G. Parkin, K. Meyer, D. O'hare, Eds.; Elsevier: Amsterdam, The Netherlands, (2022); Volume 9, pp. 263−369; (d) C. Nandi, K. Kar, A. Roy, S. Ghosh, Advances in Inorganic Chemistry, Ed. R. V. Eldik, D. Chatterjee, Elsevier, (2022); (e) D. K. Roy, S. Ghosh, J. -F. Halet, J. Cluster. Sci. 25 (2014) 225-237; (f) S. Ghosh, M. Shang, Y. Li, T. P. Fehlner, Angew. Chem. Int. Ed. 40 (2001) 1125-1127.

[24] (a) C. Nandi, A. Roy, K. Kar, M. Cordier, S. Ghosh, Inorg. Chem. 61 (2022) 16750−16759; (b) K. Geetharani, S. K. Bose, S. Sahoo, B. Varghese, S. M. Mobin, S. Ghosh, Inorg. Chem. 50 (2011) 5824−5832; (c) S. K. Bose, K. Geetharani, B. Varghese, S. Ghosh, Inorg. Chem. 50 (2011) 2445−2449; (d) K. Pathak, C. Nandi, S. Ghosh, Coord. Chem. Rev. 453 (2022) 214303; (e) D. K. Roy, S. K. Bose, R. S. Anju, B. Mondal, V. Ramkumar, S. Ghosh, Angew. Chem. Int. Ed. 52 (2013) 3222-3226; (f) S. Ghosh, A. M. Beatty, T.P. Fehlner. Collect. Czech. Chem. Commun. 67 (2002) 808-812.

[25] (a) R. Prakash, A. De, B. Kirubakaran, S. Ghosh, Inorg. Chem. 57 (2018) 14748-14757; (b) S. Kar, S. Ghosh, Borane Polyhedra beyond Icosahedron. In: Structure and Bonding, Ed. D. M. P. Mingos, Springer, Berlin, Heidelberg, (2021); Volume 187, pp. 109−138; (c) C. Nandi, S. Kar, M. Zafar, K. Kar, T. Roisnel, V. Dorcet, S. Ghosh, Inorg. Chem. 59 (2020) 3537-3541; (d) M. Zafar, S. Kar, C. Nandi, R. Ramalakshmi, S. Ghosh, Inorg. Chem. 58 (2019) 47-51; (e) S. Sahoo, S. M. Mobin and S. Ghosh, J. Organomet. Chem. 695 (2010) 945-949.

[26] S. K. Barik, V. Dorcet, T. Rosinel, J. -F. Halet, S. Ghosh, Dalton Trans. 44 (2015) 14403–14410.

[27] B. Joseph, S. K. Barik, R. Ramalakshmi, G. Kundu, T. Roisnel, V. Dorcet, S. Ghosh, Eur. J. Inorg. Chem. (2018) 2045-2053.

[28] D. Ohlmann, H. Pritzkow, H. Grutzmacher, M. Anthamattenc, R. Glaser, J. Chem. Soc., Chem. Commun. (1995) 1011-1012.

[29] G. Doyle, K. A. Eriksen, D. Van Engen, Organometallics 4 (1985) 877-881.

[30] J. C. Jeffery, F. G. A. Stone, I. Topaloglu, J. Organomet. Chem. 451(1993) 205-211.

[31] I. -H. Park, M. -S. So, K. -H. Park, Bull. Korean Chem. Soc. 28 (2007) 1515−1518.

[32] D. Sharmila, R. Ramalakshmi, K. K. V. Chakrahari, B. Varghese, S. Ghosh, Dalton Trans. 43 (2014) 9976–9985.

[33] (a) J. J. Led, H. Gesmar, Chem. Rev. 91 (1991) 1413-1426; (b) L. Yang, R. Simionescua, A. Lough, H. Yan, Dyes and Pigments 91 (2011) 264-267; (c) R. Weiss, R. N. Grimes, J. Am. Chem. Soc. 100 (1978) 1401-1405.

[34] M. J. Frisch, G. W. Trucks, H. B. Schlegel, G. E. Scuseria, M. A. Robb, J. R. Cheeseman, G. Scalmani, V. Barone, G. A. Petersson, H. Nakatsuji, X. Li, M. Caricato, A. V. Marenich, J. Bloino, B. G. Janesko, R. Gomperts, B. Mennucci, H. P. Hratchian, J. V. Ortiz, A. F. Izmaylov, J. L. Sonnenberg, D. Williams-Young, F. Ding, F. Lipparini, F. Egidi, J. Goings, B. Peng, A Petrone, T. Henderson, D. Ranasinghe, V. G. Zakrzewski, J. Gao, N. Rega, G. Zheng, W. Liang, M. Hada, M. Ehara, K. Toyota, R. Fukuda, J. Hasegawa, M. Ishida, T. Nakajima, Y. Honda, O. Kitao, H. Nakai, T. Vreven, K. Throssell, J. A. Jr. Montgomery, J. E. Peralta, F. Ogliaro, M. J. Bearpark, J. J. Heyd, E. N. Brothers, K. N. Kudin, V. N. Staroverov, T. A. Keith, R. Kobayashi, J. Normand, K. Raghavachari, A. P. Rendell, J. C. Burant, S. S. Iyengar, J. Tomasi, M. Cossi, J. M. Millam, M. Klene, C. Adamo, R. Cammi,

J. W. Ochterski, R. L. Martin, K. Morokuma, O. Farkas, J. B. Foresman, D. J. Fox, Gaussian, Inc., Wallingford CT, 2016.

[35] H. L. Schmider, A. D. Becke, J. Chem. Phys. 108 (1998) 9624−9631.

[36] EMSL Basis Set Exchange Library. https://bse.pnl.gov/bse/portal.

[37] (a) F. J. London, J. Phys. Radium 8 (1937) 397−409; (b) R. Ditchfield, Mol. Phys. 27 (1974) 789−807; (c) K. Wolinski, J. F. Hinton; P. Pulay, J. Am. Chem. Soc. 112 (1990) 8251−8260.

[38] T. P. Onak, H. L. Landesman, R. E. Williams, I. Shapiro, J. Phys. Chem. 63 (1959) 1533−1535.

[39] K. Wiberg, Tetrahedron 24 (1968) 1083–1096.

[40] (a) A. E. Reed, L. A. Curtiss, F. Weinhold, Chem. Rev. 88 (1988) 899–926; (b) F. Weinhold, C. R. Landis, Valency and Bonding: A Natural Bond Orbital Donor-Acceptor Perspective, Cambridge University Press, Cambridge, UK, 2005; (c) R. B. King, Inorg. Chem. 38 (1999) 5151–5153; (d) R. B. King, Inorg. Chim. Acta 300 (2000) 537–544.

[41] Chemcraft - https://www.chemcraftprog.com.

[42] T. Lu, F. Chen, J. Comput. Chem. 33 (2012) 580−592.

[43] (a) G. M. Sheldrick, Acta Cryst A 71 (2015) 3−8; (b) G. M. Sheldrick, SHELXS97 and SHELXL97. Program for Crystal Structure Solution and Refinement; University of Gottingen: Germany, (1997).

[44] G. M. Sheldrick, Acta Cryst. C 71 (2015) 3−8.

[45] O. V. Dolomanov, L. J. Bourhis, R. J. Gildea, J. A. K. Howard, H. Puschmann, J. Appl. Cryst. 42 (2009) 339−341.

Chart 1. Triple-decker complexes having planar 5-membered middle-deck.

Scheme 1. Syntheses of triple-decker complexes **4**-**6**.

Fig. 1. X-ray structures of **5** (left) and **6** (right). Selected bond distances (Å) and bond angles (°). **5**: B1-B2 1.69(2), Se1-B1 1.972(17), Se1-Cu1 2.387(2), Se2-Cu1 2.364(2), Se1-Co1 2.425(2), Se1-Co2 2.429(2), Se2-B2 2.015(15), Cu1-Co1 2.655(2), Cu1-Co2 2.697(2), Co2-B2 2.101(15), Co2-B1 2.176(17), Br1-Cu1 2.262(2); B1-Se1-Cu1 105.9(5), B1-Se1-Co1 58.1(5), Cu1-Se1-Co1 66.96(7), B1-Se1-Co2 58.2(5), Se1-Cu1-Co1 57.21(6), Se2-Cu1-Co1 58.13(6), Co1-Cu1-Co2 72.18(7), Se2-Cu1-Se1 96.12(8); **6**: Cu1-Se1 2.3784(16), Cu1-Se2 2.3831(15), Cu1-Br1 2.2538(14), Cu1-Rh1 2.7772(12), Cu1-Rh2 2.7659(12), Se1-Rh1 2.5343(8), Se1-Rh2 2.5410(9), Se1-B1 1.996(10), Se2-Rh1 2.5495(9), Se2-Rh2 2.5525(8), Se2-B2 2.007(9), Rh1-B1 2.266(8), Rh1-B2 2.253(8), Rh2-B1 2.238(9), Rh2-B2 2.253(8), B1-B2 1.680(13); Se1-Cu1-Se2 96.59(5), Se1-Cu1-Rh1 58.27(3), Se1-Cu1-Rh2 58.62(3), Se2-Cu1-Rh1 58.62(3), Rh2-Cu1-Rh1 76.90(3).

Fig. 2. Dihedral angles between three different planes in **5** (left) and **6** (right).

Table 1. Selected bond parameters (angles in deg and distance in Å) and ^{11}B NMR of **4**-**6**.

Fig. 3. Selected molecular orbitals of **5** and **6**. Isosurfaces are plotted at an isovalue of ± 0.045 (e/bohr^3)$^{1/2}$.

Table 2. $\nabla^2\rho(r)$ (Laplacian of the electron density), energy density (H(r)), and ELF (electron localization function) values at the bond critical points (BCPs) computed at the BP86/ def2-TZVP level of theory of selected bonds in **5** and **6**.

Fig. 4. Contour line diagrams of the $\nabla^2 \rho(r)$, Laplacian of the electron density, of (a) Co2-B1-B2 and (b) Cu1-Se1-B1-B2-Se2 planes for **5**. Solid red lines indicate areas of charge concentration ($\nabla^2 \rho(r) < 0$), while solid black lines show areas of charge depletion ($\nabla^2 \rho(r) > 0$). BCPs (bond critical points) are indicated by blue dots.

Chart 1.

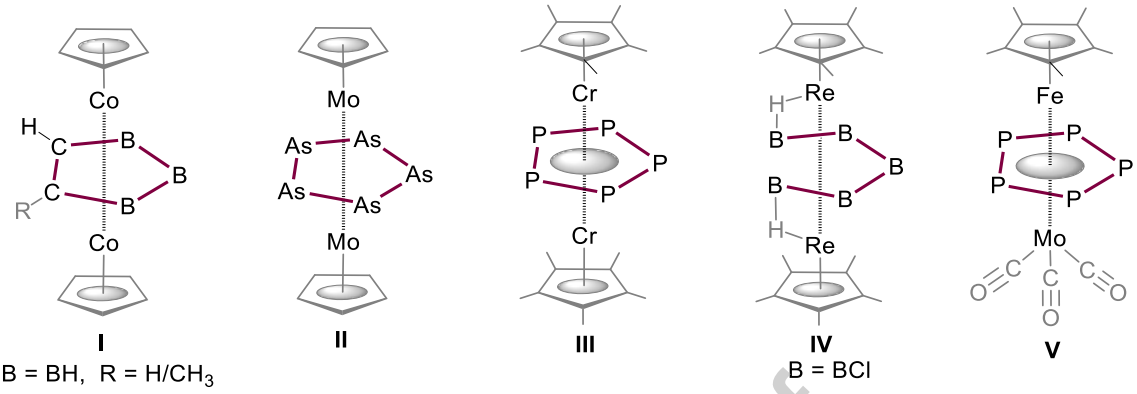

Scheme 1.

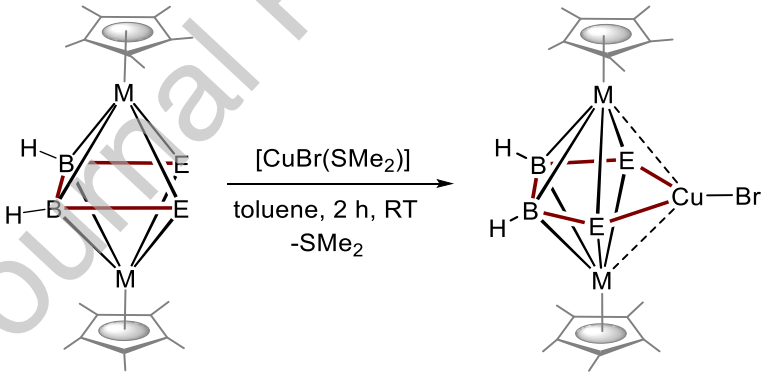

1: M = Co, E = S
2: M = Co, E = Se
3: M = Rh, E = Se

4: M = Co, E = S
5: M = Co, E = Se
6: M = Rh, E = Se

Fig. 1.

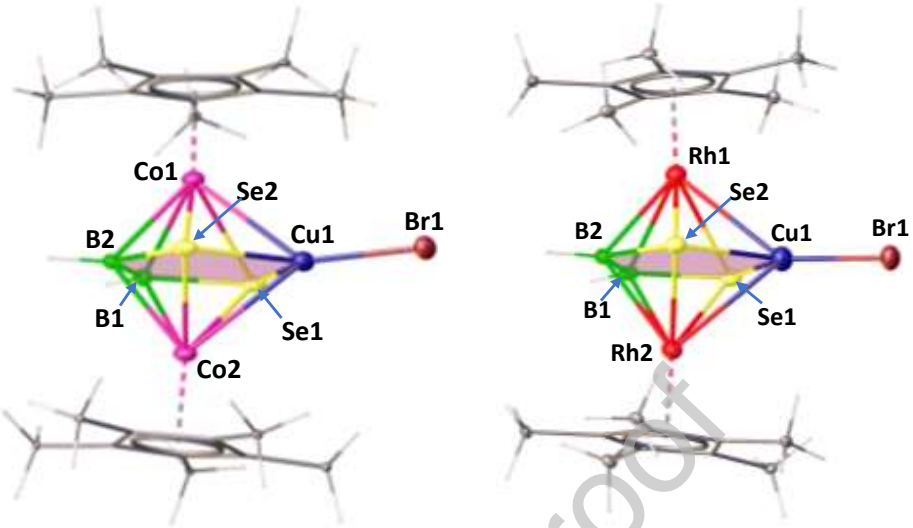

Fig. 2.

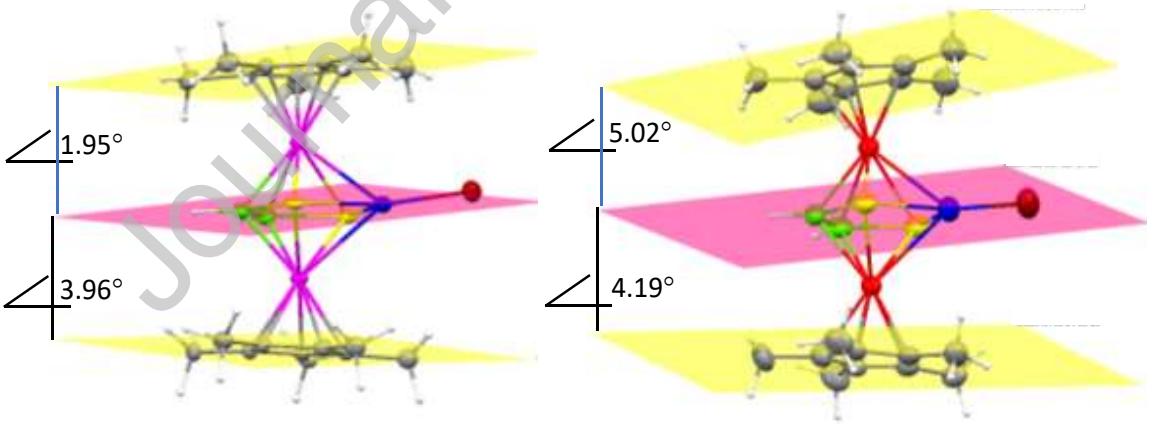

Table 1.

Table1. Selected bond parameters (angles in deg and distance in Å) and ^{11}B NMR of **4**-**6**.

Triple-decker Complexes	Structural Parameters				^{11}B NMR (δ, ppm)	
	d[B-E][a]	d[B-B][a]	d(M-Cu)[a]	dihedral angle[b]	Expt.	Calc.
4	-[c]	-[c]	-[c]	-[c]	20.0	16.0
5	1.993	1.690	2.676[d]	3.96, 1.95	18.1	24.1
6	2.001	1.680	2.771[e]	5.02, 4.19	18.3	16.3

[a] Average distance in Å, [b] Cp* and B_2E_2Cu ring, [c] data not available, [d] M = Co, [e] M = Rh

Fig. 3.

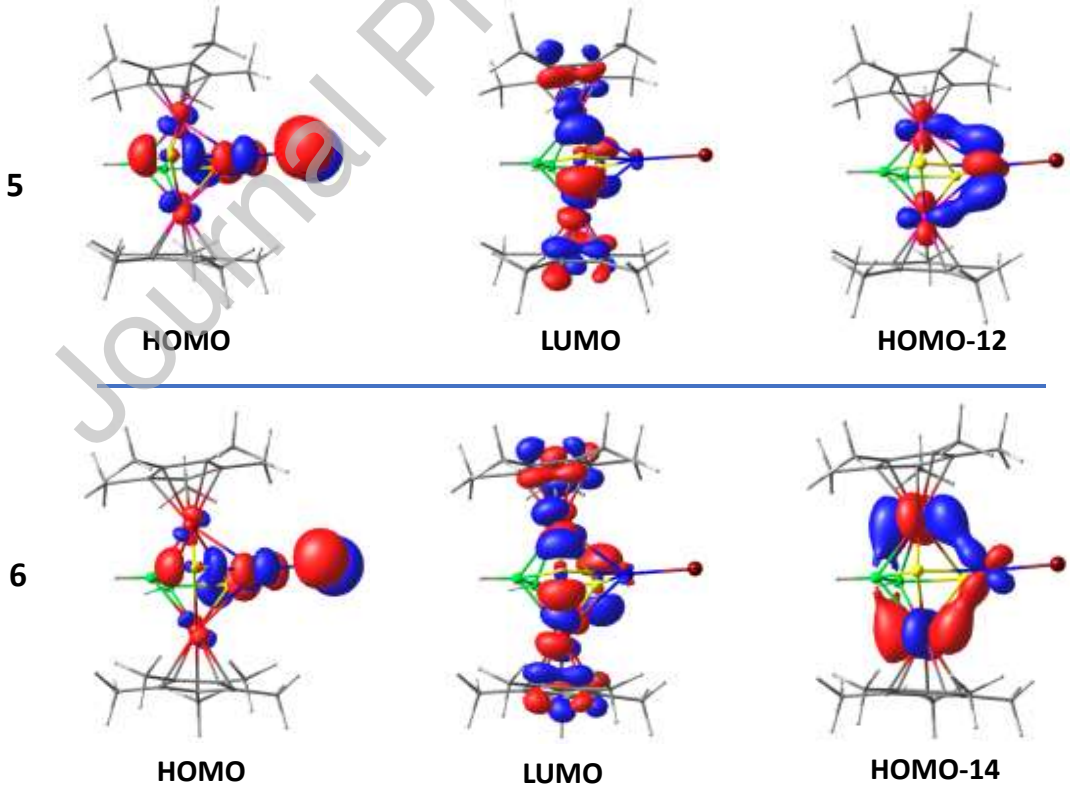

Table 2.

	5			**6**		
bond	$\nabla^2\rho(r)$	H(r)	ELF	$\nabla^2\rho(r)$	H(r)	ELF
B-B	-0.2280	-0.09167	0.9027	-0.2102	-0.0856	0.8992
B-Se	-0.1467	-0.08170	0.7473	-0.1411	-0.0772	0.7588
Se-Cu	0.1433	-0.0159	0.2531	0.1397	-0.0149	0.2497
Cu-Br	0.2017	-0.0218	0.2291	0.2002	-0.0212	0.2272
M-Cu[a]	0.0488	-0.0639	0.2324	0.0553	-0.0581	0.2127
M-Se[a]	0.1250	-0.0146	0.2583	0.1234	-0.0128	0.2862
B-B-M[a]	0.0906	-0.0230	0.4313	0.0781	-0.0237	0.4742

[a] M = Co for **5**; M = Rh for **6**

Fig. 4.

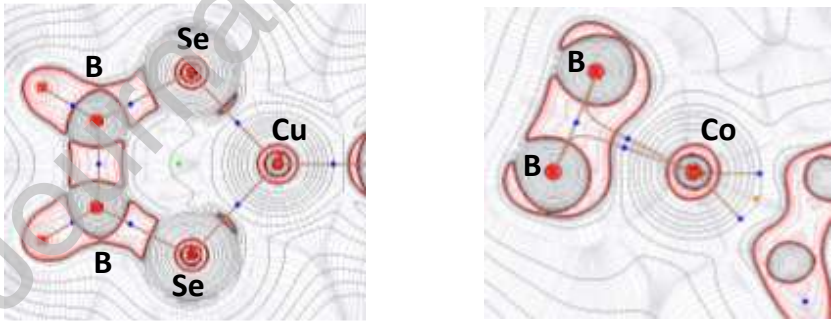

(a) **(b)**

Notes

The authors declare no competing financial interest.

Table of Contents Entry